

**MAGNETOPHORETIC MIGRATION OF  
MAGNETIC NANOPARTICLES THROUGH  
CELLULOSE MATRIX**

**MUHAMMAD SUFIAN BIN MOHD SALLEH**

**UNIVERSITI SAINS MALAYSIA**

**2021**

**MAGNETOPHORETIC MIGRATION OF  
MAGNETIC NANOPARTICLES THROUGH  
CELLULOSE MATRIX**

by

**MUHAMMAD SUFIAN BIN MOHD SALLEH**

**Project submitted in fulfilment of the requirements  
for the degree of  
Bachelor of Chemical Engineering**

**June 2021**

## ACKNOWLEDGEMENT

It is my highest pleasure to find a great chance to be supervised by Prof. Lim Jit Kang. I would like to thank Prof. for his guidance throughout the journey to complete this report, who has continuously shared his knowledge and guided me tirelessly. It was a great privilege and honour to work under his guidance. I am beyond grateful for what he has offered me.

My sincere thanks also go to my friends for the discussions, for the sleepless nights working together rushing for deadlines, for their constant encouragement, and for all the fun we have had in the last four years. I express my warmest thanks to the School of Chemical Engineering staff and community for the genuine support and cooperation throughout this research work.

Besides, I would like to express my deep and sincere gratitude to my family members: my parents Mohd Salleh and Siti Zubaidah, for giving birth to me in the first place and encouraged me spiritually throughout my study years in USM. Also, not to forget my siblings, who keep cheering me up when I needed them the most especially my twin brother, Muhammad Safwan. Lastly, thank you for Wai Hong Chong and Wei Ming Ng as my post-graduate supervisors for this final year project for their knowledge and guidance.

## TABLE OF CONTENTS

<b>ACKNOWLEDGEMENT</b>	<b>i</b>
<b>TABLE OF CONTENTS</b>	<b>ii</b>
<b>LIST OF TABLES</b>	<b>iv</b>
<b>LIST OF FIGURES</b>	<b>v</b>
<b>LIST OF SYMBOLS</b>	<b>vii</b>
<b>LIST OF ABBREVIATIONS</b>	<b>viii</b>
<b>LIST OF APPENDICES</b>	<b>ix</b>
<b>ABSTRAK</b>	<b>x</b>
<b>ABSTRACT</b>	<b>xi</b>
<b>CHAPTER 1 INTRODUCTION</b>	<b>1</b>
1.1 Background	1
1.2 Problem Statement	6
1.3 Objectives	7
<b>CHAPTER 2 LITERATURE REVIEW</b>	<b>8</b>
2.1 Magnetophoresis	8
2.1.1 Effect of Particle Size on Magnetophoresis	10
2.1.2 Effect of Linked Media on Magnetophoresis	11
2.2 Drag Force	11
2.3 Velocity Prediction in Confined Space	14
2.4 Colloidal Stability	16
2.5 Capillary and Steric Force	17
<b>CHAPTER 3 METHODOLOGY</b>	<b>19</b>
3.1 Materials	19
3.2 Overview of Research Methodology	19
3.3 Design of Experiment	22

3.4	Velocity calculation	23
3.5	Drag force calculation	25
3.6	Preparation of PSS-Coated and Naked MNPs	28
3.7	Record the magnetophoretic dragging phenomena	31
3.8	Thesis and report writing	31
<b>CHAPTER 4 RESULTS AND DISCUSSION</b>		<b>32</b>
4.1	Capillary Force as Baseline	32
4.2	Magnetophoresis of naked MNPs for 100 mg/L through grade 4 paper	36
4.3	Magnetophoresis of naked MNPs for 500 mg/L through grade 4 paper	41
4.4	Magnetophoresis of PSS 70k-coated MNPs through grade 4 paper	45
4.5	Magnetophoresis of PSS 70k-coated MNPs through grade 5 paper	48
4.6	Effect of magnetic field on the magnetophoresis	52
4.7	Sustainability	54
<b>CHAPTER 5 CONCLUSION AND FUTURE RECOMMENDATIONS</b>		<b>55</b>
5.1	Conclusion	55
5.2	Recommendations	56
<b>REFERENCES</b>		<b>57</b>
APPENDICES		

## LIST OF TABLES

	<b>Page</b>
<b>Table 1.1:</b> Applications of magnetophoresis	3
<b>Table 2.1:</b> Drag coefficient correlations for a spherical particle at low and high particle Reynolds numbers	12
<b>Table 3.1</b> Properties of Whatman grade paper	23
<b>Table 3.2:</b> Parameters of MNPs from published literature	23
<b>Table 3.3:</b> Summary of the velocity and drag force values calculated in this work and by other authors under different conditions	27
<b>Table 4.1</b> Total number of MNPs at the specific distance	35
<b>Table 4.2</b> Area covered by PSS-coated MNPs on grade 4(%)	47
<b>Table 4.3</b> Area covered by PSS-coated MNPs on grade 5(%)	50
<b>Table 5.1</b> captured images of Naked MNPs on grade 4 paper	61
<b>Table 5.2</b> Captured images of 500 mg/L Naked MNPs on grade 4 paper	62
<b>Table 5.3</b> captured images of PSS-coated MNPs on grade 4 paper	63
<b>Table 5.4</b> captured images of PSS-coated MNPs on grade 5 paper	64
<b>Table 5.5</b> captured images of PSS-coated MNPs on grade 4 paper (bar magnet)	65

## LIST OF FIGURES

	<b>Page</b>
<b>Figure 3.1</b> Flow diagram of research project on magnetophoresis of MNPs through cellulose matrix	21
<b>Figure 3.2:</b> Top view of the experiment set up	23
<b>Figure 4.1</b> Overview of the baseline design of the experiment driven by capillary force	33
<b>Figure 4.2</b> Microscopic view of naked MNPs for 100 mg/L at 0 cm	34
Figure 4.3 No. of MNPs against distance for 5 different conditions of experiment driven by capillary force	35
<b>Figure 4.4</b> Naked MNPs on grade 4 at 0.5 cm (a) MNPs distribution of baseline (b) MNPs distribution after 15 s	36
<b>Figure 4.5</b> No. of MNPs against distance for magnetophoresis of naked MNPs on grade 4 paper	38
<b>Figure 4.6:</b> Distribution of Naked MNPs after 60 s at 1.0 cm with 100 mg/L	40
<b>Figure 4.7</b> Microscopic view of MNPs distribution at 0 cm for 500 mg/L after 15 s magnetophoresis	42
<b>Figure 4.8</b> Mean diameter ( $\mu\text{m}$ ) against distance (cm) for 500 mg/L of naked MNPs	44
<b>Figure 4.9</b> Microscopic view of cluster MNPs at 1.0 cm after 15 s of magnetophoresis	44
<b>Figure 4.10</b> No. of MNPs against distance (cm) for 70k PSS-coated MNPs	46
<b>Figure 4.11</b> Area covered (%) against distance (cm) for PSS coated MNPs on grade 4	48
<b>Figure 4.12</b> Comparison in microscopic view of cellulose matrix structure a) Cellulose matrix of grade 5 b) Cellulose matrix structure of grade 4	49

<b>Figure 4.13</b> No. of particles against distance (cm) for PSS-coated MNPs on grade 5 paper	50
<b>Figure 4.14</b> covered (%) against distance (cm) for PSS coated MNPs on grade 5	51
<b>Figure 4.15</b> No. of particles against distance (cm) for PSS-coated MNPs on grade 4 paper with bar magnet	52



## LIST OF SYMBOLS

$\mu_0$	Permeability
A	Area submerged particle/object
$C_D$	Drag Coefficient
Cr	Chromium
$D_p$	Diameter of the particle
$F_d$	Drag force
$F_g$	Gravitational force
$F_m$	Magnetic force
g	Gravitational acceleration
$H_a$	Magnetic field intensity
$M_n$	Manganese
$M_p$	Magnetization of the particle
$M_s$	Saturation magnetic moments
$NO_2$	Nitrogen Oxide
r	Radius of the particle
$Re$	Reynold's number
v	Velocity of the particle
$V_p$	Volume of the particle
$\gamma\text{-Fe}_2\text{O}_3$	Sigma iron oxide
$\eta$	Dynamic viscosity
$\rho$	Density
$\rho_f$	Density of the fluid
$\rho_p$	Density of the particle
$\zeta$	Langevin Function

## LIST OF ABBREVIATIONS

DNA	Deoxyribonucleic acid
DEP	Dielectrophoresis
ECM	Extracellular matrix
ffPADs	Fast flow microfluidic paper-based analytical devices
FFF	Fluid Flow Fractionation
GAGs	Glycosaminoglycans
HGMS	High Gradient Magnetic Separation
LOC	Lab on a Chip
LGMS	Low gradient magnetic separation
MNPs	Magnetic Nanoparticles
MARIA	magnetic relaxation anisotropy
$\mu$ TAS	Micro total analysis
$\mu$ PADs	Microfluidic paper based analytical devices
NPs	Nanoparticles
PDDA	poly (diallyl dimethylammonium chloride)
PSS	poly (sodium (4) styrene sulfonate)
VDWs	Van Der Waals

## **LIST OF APPENDICES**

Appendix A      TABLE OF CAPTURED IMAGES

# MAGNETOPHORETIC MIGRATION OF NANOPARTICLES THROUGH CELLULOSE MATRIX

## ABSTRAK

Migrasi nanopartikel magnetik (MNP) melalui matriks selulosa telah dikemukakan dalam tesis ini. Eksperimen ini dijalankan untuk mengkaji pengaruh kestabilan koloid, pengagregatan MNP, kepekatan, ukuran pori matriks selulosa dan kekuatan medan magnet pada magnetoforesis MNP melalui struktur selulosa yang kompleks. Magnetite,  $\text{Fe}_3\text{O}_4$  digunakan sebagai MNP untuk mempelajari magnetoforesis di bawah mikroskop Optik. Semua gambar fenomena magnetoforetik yang diambil dianalisis dengan menggunakan NIH ImageJ. Satu set percubaan yang sederhana dilakukan dengan meletakkan magnet 2 cm dari titik awal MNP disuntik pada kertas kromatografi Whatman. Berdasarkan eksperimen yang dijalankan, 100 mg / L MNP bersalut polyelectrolyte poli (sodium (4) styrene sulfonate) (PSS) dapat berhijrah melalui kertas gred 4 setelah 30 dan 60 s magnetoforesis dengan 0.007492% dan 0.0162% kawasan yang diliputi masing-masing pada 2 cm. Bagi MNP tulen dengan keadaan yang sama, kawasan yang dilindungi selepas 30 dan 60 s masing-masing adalah 0 dan 0,00133%. Didapati bahawa kawasan yang diliputi untuk pergerakan magnetoforetik MNP melalui kertas gred 5 lebih rendah daripada kertas gred 4, sedangkan pada jarak 1.5 dan 2 cm kawasan yang diliputi masing-masing adalah 0.00245% dan 0.00294%. Selain itu, kepekatan larutan MNP yang lebih tinggi akan menghadkan magnetoforesis MNP melalui matriks kerana pembentukan agregasi yang menghalang pergerakan zarah dari melewati liang matriks selulosa.

# MAGNETOPHORETIC MIGRATION OF NANOPARTICLES THROUGH CELLULOSE MATRIX

## ABSTRACT

The migration of magnetic nanoparticles (MNPs) through cellulose matrix has been presented in this thesis. The experiment was carried out to study the influence of colloidal stability, aggregation of MNPs, concentration, the pore size of the cellulose matrix, and strength of magnetic field on the magnetophoresis of MNPs through the complex structure of cellulose. Magnetite,  $\text{Fe}_3\text{O}_4$  were used as the MNPs to study the magnetophoresis under an Optical microscope. All the captured images of the magnetophoretic phenomena were analysed by using NIH ImageJ. A simple setup of the experiment was done by placing a magnet 2 cm away from the initial point of MNPs was injected on the Whatman chromatography paper. Based on the experiments conducted, 100 mg/L of poly (sodium (4) styrene sulfonate) polyelectrolyte (PSS) coated MNPs were able to migrate through grade 4 paper after 30 and 60 s of magnetophoresis with 0.007492 % and 0.0162 % of the area covered at 2 cm, respectively. As for naked MNPs with the same conditions, the area covered after 30 and 60 s is 0 and 0.00133 % respectively. It was found that the area covered for the magnetophoretic motion of MNPs through grade 5 paper was lower than grade 4 paper, whereas at 1.5 and 2 cm the area covered is 0.00245 % and 0.00294 % respectively. Besides, a higher concentration of MNPs solution will limit the magnetophoresis of MNPs through the matrix due to the formation of aggregation that inhibits the motion of the particles from passing through the pore of the cellulose matrix.

# **CHAPTER 1**

## **INTRODUCTION**

Chapter 1 introduces the overview of this research and the significance of magnetophoresis in the field of fluid flow fractionation (FFF). In general, this chapter summarizes the research background of magnetophoretic migration of magnetic nanoparticles, the problem statements, and the objectives of this final year project.

### **1.1 Background**

Magnetophoresis has gathered significant interest within the scientific community in recent years because of the continuous growth of new magnetic particles that were invented for various applications which composed of drug delivery, the removal of heavy ions from water, the removal of microalgae, and many more (Leong et al., 2020). Because of its cost-effectiveness, simplicity in terms of application as well as biocompatible (Alnaimat et al., 2018), magnetophoresis has gained much attraction mainly due to its feasibility as an alternative to current technologies.

Compared to magnetophoresis, acoustophoresis is usually ineffective when it is handling particles from sub-micrometres for focusing purposes and segregation. Besides, problems with heating can be found during long-term operations affecting the acoustophoresis applicability for biomedical applications (Adams et al., 2012). Acoustophoresis can be defined as the migration with sound in which the phenomenon of manipulating microparticles by using acoustic force. Another than that, limitation of another phenomenon is electrophoresis are microparticles need to be charged since electrophoresis cannot manage electrically neutral particles, migration time for the microparticles is not rapid and limited to separation applications (Alnaimat et al.,

2018). Another driven control scheme is Dielectrophoresis (DEP) in which DEP uses dielectric forces for the manipulation of particles especially living cells by Interaction of components of dielectric polarisation induced by the electrical field in the particles with spatial inhomogeneities in the field (Gascoyne & Vykoukal, 2002). The disadvantage of DEP is limited applicability to cell handling applications as it is exposed to a similar high electrical field. It has been reported that the amount of publications on magnetophoresis has increased rapidly over the past 10 years because of the grow interest in its applications especially in biomedical research and clinical diagnostics and therapy (Webster, 1999)

Some several applications and technologies have been developed based on magnetophoresis such as Lab-on-a-Chip (LOC). LOC technologies have represented a real breakthrough in the field of in vitro biochemical and biological analysis in recent decades. LOC or also known as the micro total analysis system ( $\mu$ TAS) is the advanced microsystem that applies mechanical, electronic, and fluidic functions for the mixing, pumping, and manipulating system purposes. LOC system has various applications such as extraction of Deoxyribonucleic acid, DNA, manipulation of cells, and drug testing. (Iacovacci et al., n.d.) in their study on magnetophoresis for LOC, applications have mentioned that magnetic-field-based strategies exploitation can be a good solution to manipulate and liquids/particles mixing at the microscale due to the low Reynolds numbers and the effect of capillary forces in the system. Other than that, the authors mentioned the non-contact manipulation of magnetophoresis can be a good advantage in the applications. Besides, the sources of the magnetic field are close to the working environment, hence compensate for the rapid decay of magnetic force between the source and the object with the distance.

Another recent application of magnetophoresis is the removal of microalgae from culture media by low-gradient magnetic separation (LGMS) that have been studied by (Lim et al., 2012). Iron oxide nanoparticles are binding to the microalgal cells (*Chlorella sp.*) through either two methods which are immobilized-on or attached-to strategy via electrostatic interaction. It has been reported that the immobilized-on strategy shows a higher removal efficiency compared to the common attached-to technique due to the two factors which are first is because of agglomeration of the NPs and formation of nanoclusters before attachment to the microalgal cells and secondly due to the cluster formation of microalgal cells by poly (diallyl dimethylammonium chloride) (PDDA) because of the bridging flocculation-induced. A removal efficiency can be achieved up to 99% of the microalgal cells by applying the immobilize-on strategy. Several applications that have been developed that applied magnetophoresis are tabulated in **Table 1.1**.

**Table 1.1:** Applications of magnetophoresis

Application	Field	Reference
Drug delivery	Medicine	(Kumar & Murthy, 2016)
Heavy iron removal	Water treatment	(Dave & Chopda, 2014)
Cancer progression monitoring	Medicine	(Park et al., 2015)
Tissue engineering	Medicine	(Yaman et al., 2018)
Arsenic removal	Water treatment	(Slovaca, 2012)

Since we are dealing with the linked media of cellulose in this thesis, it is crucial to understand the structure of this intertwined structure of cellulose to predict the movement of magnetic nanoparticles (MNPs) in the complex linked media. The term “magnetic nanoparticles” (MNPs) specify those nanoparticles (NPs) that display certain responses to an applied magnetic field (Issa et al., 2013). The composition of these structures contributes to the physical and chemical complexity of the nanoparticles involved in traveling through the media (L.O. Mair, 2015). The structure



of cellulose consists of a crystalline structure of thousands of units that are formed by glucose molecules. The structure of cellulose can be defined as a long-chain polymer with a huge molecular weight ( $<500,000$ ) and a high degree of polymerization ( $<10,000$ ). Cellulose is the main component of cell walls in biomass with the molecular formula  $(C_6H_{10}O_5)_n$  (Basu, 2018).

Few properties need a thorough understanding to help us to study the magnetophoresis of nanoparticles through cellulose matrix since the matrix of cellulose is not a freely suspended solution, instead, it is an interlinked media. The dynamical behavior of MNPs inside cellulose matrix needs to investigate for the development of MNPs-Cellulose matrix integrated sensing system. The dynamical behavior of MNPs that experienced magnetophoresis inside cellulose matrix such as Reynold numbers, drag force, and viscosity of the fluid are discussed in this thesis. In this work, we are focused on the migration of MNPs through cellulose matrix which is chromatography paper by using magnetic force and improve the working conditions for the magnetophoretic motion of MNPs, Because the process of separating MNPs can be tedious, microfluidic platforms were chosen to automate and simplify the migration process (Call et al., 2020). Magnetophoresis is one of the notorious microfluidic platforms whereby particles/cells separated in a continuous flow using a permanent magnet to move ferromagnetic materials/labeled cells from one flowing stream to another (Yaman et al., 2018). In this thesis, the project mainly demonstrates magnetophoresis of MNPs on chromatography paper and optimizes its capabilities by manipulating the conditions of MNPs and their conditions.

Many in vivo applications of superparamagnetic magnetite ( $Fe_3O_4$ ) nanoparticles have been studied, including magnetic targeting drug delivery, magnetic fluids intracellular hyperthermia, and magnetic resonance imaging contrast

enhancement (X. Q. Xu et al., 2006). One of the factors magnetite are widely used in many applications is because of their ease of synthesis across a range of controllable sizes and their biocompatibility (Lim et al., 2009). To improve the colloidal stability of nanoparticles, the surface of nanoparticles could be modified with a polymer such as poly(ethylene oxide) and poly(acrylic acid) (Moore et al., 2015).

Recently a paper-based magnetophoresis experiment has been conducted by(Call et al., 2020) applying a fast flow microfluidic analytical system in their experiment to separate/isolate the cells from complex matrices for analysis. The system based on a pump-free microfluidic device ( $\mu$ PAD) has succeeded to isolate the MNPs with high capture efficiency regardless of the concentrations used.  $\mu$ PAD are biocompatible for a variety of applications including clinical diagnosis, food quality control, and environmental monitoring, and have numerous advantages over traditional microfluidics, such as porosity-induced capillary action eliminates the need for an external pump (Fratzl et al., 2018).

## 1.2 Problem Statement

Magnetophoresis (migration process of nanoparticle in response, relative to surrounding) of nanoparticles in response to an externally applied magnetic field has been widely used as the working mechanism for various separation processes. In the freely suspended solution, the separation kinetics of the magnetic nanoparticles (MNPs) under magnetophoresis is mainly dictated by the particle size and field gradient. Whilst moving through a highly linked media, such as cellulose matrix, the motion path of the MNPs become much more complicated and is relying heavily on overcoming the fluid resistance imposed by the surrounding fluid of MNPs and these intertwined structures. Such fluid flow behavior is unique and belongs to the domain of low Reynold number flow. One of the fundamental requirements for a successful micro total analysis system is the ability to fractionate and isolate target cells and particles from the sample. Flow fractionation has a higher potential than particle-cellulose sensing due to the advantages of magnetophoresis on the choice of device construction material as magnetic fields can penetrate most materials of choice such as polymers. Furthermore, magnetic forces are such a strong force that make it a long-range force with the gentle and non-destructive for the particles, particles are easy to manipulate inside the micro-channels by applying an external magnetic field, and by applying magnetoresistance of magnetic relaxation anisotropy (MARIA) technique, the particles and the biological attached can be easily detected. In this thesis, numerical values for drag force and velocity of the MNPs that experienced magnetophoresis through the cellulose matrix will be calculated. The calculated data will then be compared and validated with experimental results from published literature.

### **1.3 Objectives**

- I. To record the magnetophoretic dragging phenomenon of MNPs through cellulose matrix
- II. To identify the best working conditions for the magnetophoretic motion of MNPs through cellulose matrix
- III. To study the effect of colloidal stability for the magnetophoretic motion of MNPs through cellulose matrix

## CHAPTER 2

### LITERATURE REVIEW

#### 2.1 Magnetophoresis

Magnetophoresis can be described as the movement of magnetic particles, relative to their surrounding fluid, under the influence of an externally imposed magnetic field gradient (Leong et al., 2020). The interesting characteristic of magnetophoresis such as under the right-controlled conditions, it is gentle and non-destructive for biological analyses of protein and magnetophoresis is applicable for huge protein complexes. Other than that, compare to other forces, magnetic forces can be much stronger that makes it a long-range force correspond to other active manipulation techniques (Alnaimat et al., 2018). The magnetophoresis is mainly influenced by the three gravitational forces ( $F_g$ ), magnetic ( $F_m$ ), and drag ( $F_d$ ). These forces will determine the direction and velocity of the motion of the particles in a gradient magnetic field (Yan & Wu, 2013). The force balance equation in magnetophoresis is described as

$$F_m + F_g + F_d = 0 \quad (1)$$

In which Equation 2

$$F_m = \mu_o V_p \rho_p (M_p \circ \nabla) H_a \quad (2)$$

$$F_g = \frac{4}{3} \pi r^3 (\rho_p - \rho_f) g \quad (3)$$

$$F_d = -6\pi\eta r v \quad (4)$$

In equation (2),  $\mu_o$  is the permeability of free space ( $4\pi \times 10^{-7} \text{H/m}$ ),  $V_p$  and  $M_p$  are the volume and magnetization of the particle,  $\rho_p$  is particle density and  $H_a$  is referring to the applied magnetic field intensity at the centre of the particle. Where  $r$  in the equations (3) and (4) is the radius of the particle;  $\rho_p$  and  $\rho_f$  are the particle and fluid density

respectively in the unit ( $\text{kg/m}^3$ );  $g$  is the gravitational acceleration ( $9.81 \text{ m/s}^2$ );  $\eta$  is the dynamic viscosity of separation fluid ( $\text{kg/ms}$ ) and finally  $v$  represents the velocity of the particle ( $\text{m/s}$ ). The negative symbol in equation (4) indicates the opposite direction of drag force experienced by the particle with its velocity inside the cellulose matrix. During magnetophoretic transport through the homogenous Newtonian fluid inside of a linked media such as cellulose matrix, magnetic particle experienced few forces that are composed of magnetic force by the permanent magnet, drag force imposed by the surrounding liquid, and additional steric force that imposed by the matrix fibers (L.O. Mair, 2015).

The intrinsic spin of electrons and their orbital motion around the nucleus caused magnetism in materials. Based on their response to a magnetic field, materials can be classified into three which are diamagnetic, paramagnetic, and ferromagnetic materials. Nonmagnetic materials are classified as diamagnetic for example biological cells, water, and plastic (Alnaimat et al., 2018). Due to the incomplete cancellation of electron spin and orbital magnetic moment in paramagnetic materials, a permanent magnetic dipole moment exists. The dipole moments are oriented randomly in the absence of an applied field, so there is no net macroscopic magnetization in the material (Kotnala & Shah, 2015). Individual magnetic dipole moments align themselves in the direction of the magnetic field if their atoms or molecules align themselves in the direction of the magnetic field, causing them to be attracted to the magnetic field. Examples of paramagnetic materials such as Chromium (Cr), manganese (Mn), and  $\text{NO}_2$  in which these materials show weak attraction in the presence of magnetic field. In the absence of an external magnetic field, dipolar interactions in ferromagnetic materials promote a parallel alignment of the magnetic dipole vectors, resulting in a material with a net

magnetization. This alignment of magnetic moments, however, does not imply that a ferromagnetic compound is magnetic (Spain & Venkatanarayanan, 2014).

### **2.1.1 Effect of Particle Size on Magnetophoresis**

Generally, the size of the magnetic nanoparticles (MNPs) are crucial in magnetophoresis as magnetophoretic property and magnetic of MNPs are highly reliant on its size (Vestal & Zhang, 2002). Size fractionation of nanoparticles using a low-gradient magnetic separation (LGMS) have been studied by (Yeap et al., 2014) in which the experiments were conducted by using Poly (sodium 4-styrenesulfonate) (PSS)-grafted iron oxides NPs (average hydrodynamic size at 200 nm) and bare iron oxide,  $\text{Fe}_3\text{O}_4$ . The authors observed that the magnetophoresis profiles were significantly decayed and declined gradually before it reaches a steady state where it is expected  $\text{Fe}_3\text{O}_4$  clusters of larger size formed at higher concentration undergo more rapid magnetophoretic separation than smaller clusters formed at low concentration. Different observation with the PSS-grafted  $\text{Fe}_3\text{O}_4$  where the magnetophoresis for these macromolecules is much slower compared to the bare  $\text{Fe}_3\text{O}_4$ . The smaller NPs, the easier they will reach the centre of the walls by diffusion (Liot et al., 2018). MNPs that are smaller than the average pore size of the chromatography paper will be retained within the cellulose matrix resulting in no migration of MNPs through the cellulose matrix. A study of three different sizes of MNPs had conducted by (Call et al., 2020) on Whatman 1 chromatography paper that has an average pore size of 11  $\mu\text{m}$ . It was observed that 2  $\mu\text{m}$  and 8  $\mu\text{m}$  MNPs were retained within the paper fibres while 44.1  $\mu\text{m}$  MNPs were observed migrated across the paper fibres towards the source of magnetic field or in this context is cellulose matrix.

### **2.1.2 Effect of Linked Media on Magnetophoresis**

(L.O. Mair, 2015) who study about the single particle tracking of particles that experienced through the extracellular matrix (ECM) found that, smaller particle obtained larger velocities even though experienced smaller magnetic force. MNPs have trouble traveling through linked media such as ECM since it is composed primarily of collagen, laminin, and glycosaminoglycans (GAGs) that influencing the physical and chemical complexity of the matrix. Inside the interlinked media, apparent viscosity experienced by larger diameter is larger than smaller viscosity due to steric hindrance from the matrix that is experienced by the particles as they move along the matrix. The study also observed that smaller MNPs experienced large path deviations normal to the field gradient, being less magnetically confined and show remarkably larger variation in orientation angle to the magnetic field. The observation of the MNPs that experienced magnetophoresis in this study will help for considering the size of NPs that will be used in this thesis to provide the best working conditions for MNPs that experience magnetophoresis through cellulose matrix. The majority of suspended MNPs will be retained or trapped in the cellulose matrix if fluid velocities are above 1.5 cm/s and lower than 0.5 cm/s (Call et al., 2020). The phenomena were observed for fast flow microfluidic paper-based fiber (ffPADs) in which the device was driven by capillary action in a gap between stacked layers of paper and transparency sheets to drive the flow of the MNPs solution at higher velocity compared to the traditional microfluidic paper-based analytical devices ( $\mu$ PADs).

## **2.2 Drag Force**

One of the key factors in determining the dynamics of solid bodies that move in a viscous fluid is drag force. For the spherical particles that are moving in a viscous fluid, drag force represents the total resistive force applied by the surrounding fluid on



the particle surface in which the force influences the velocity of the particle, hydrodynamic size of the particle, and the physical properties of the fluid (Yarin, 2012). Two assumptions need to consider using the fundamental equation of the drag force in a viscous fluid. Firstly, a particle's drag is approximately directly proportional to the unperturbed fluid velocity. Then, the force is taken to be the same in magnitude but opposite to the drag particle in the direction in which the disturbance generated by a particle must be approximated by the force of a point at the centre of the spherical particle (Tam, 1969).

Equation (4) is also known as Stoke's law and it can be shown using dimensionless drag coefficient  $C_D$  as

$$F_d = A \left( \frac{1}{2} \rho_f v^2 \right) C_D \quad (5)$$

where  $A$  is the area of the submerged object. Since the MNPs inside the cellulose matrix are spherical,  $A$  can be calculated as  $\pi r^2$ . The drag coefficient,  $C_D$  for a spherical particle depends on the Reynold number and can be expressed as

$$C_D = \frac{24}{Re} \quad (6)$$

Equation (6) only valid for the Reynold numbers  $Re \leq 0.1$  (Yarin, 2012). For Reynold numbers higher than 0.1, several correlations have been suggested to determine an analytical solution for the drag coefficient. The correlations are tabulated in **Table 2.1**.

**Table 2.1:** Drag coefficient correlations for a spherical particle at low and high particle Reynolds numbers

Reference	Correlation	Re - range
(Yarin, 2012)	$C_D = \frac{24}{Re} (1 + 0.15Re^{0.687})$	$1 < Re < 800$
(Kinaci, 2015)	$C_D = \frac{24}{Re} + \frac{3}{\sqrt{Re}} + 0.34$	$Re < 10^4$

(Kinaci, 2015)

$$C_D = \left( \sqrt{\frac{24}{Re}} + 0.5407 \right)^2$$

Re < 6000

---

Reynold number is applied to identify the conditions of flow over a spherical particle in which the concept is described as particle Reynold number. The particle Reynold numbers for Newtonian fluid in cellulose matrix is expressed as

$$Re = \frac{\rho_f v D_p}{\eta} \quad (7)$$

In which  $D_p$  is the diameter of the particle (Kinaci, 2015). Due to a highly linked media structure possessed by cellulose matrix, the motion path of the MNPs becomes much more complicated and belongs to the domain of low Reynold numbers.

(Gómez-Pastora et al., 2019) in their study found that the approximate value of drag force for the particles that experienced magnetophoresis in a microchannel of viscous fluid is 1.65 nN. The simulations were conducted with the properties of 5 $\mu$ m of sphere bead diameter, 2000 kg/m<sup>3</sup> of bead density, and 10.5 A/m of magnetization saturation. From the drag coefficient used in their study, it is believed that the Reynold numbers for the fluid flow inside the microchannel are  $Re < 2.10^5$ . However, the drag force is assumed negligible for the NPs after reaching the channel wall due to the laminar flow regime (fluid velocity approaching zero) and NPs experienced high magnetic force at that point.

Low gradient magnetic separation (LGMS) is the separation conducted by weak magnetic field gradients created by permanent magnets have studied by (Leong et al., 2020). From the data obtained in the literature, the drag force of small superparamagnetic nanoparticles ( 12 nm  $\gamma$ -Fe<sub>2</sub>O<sub>3</sub> ) with the low beads (NPs coated with silica) density of 1020 kg/m<sup>3</sup> and 1200 kg/m<sup>3</sup> for high-density beads is 0.000322 pN (calculated by using equation(4)) The maximum saturation magnetization in their

study is 68 A m<sup>2</sup>/kg in which the magnetophoretic velocity of the particles is approximately at 0.16 μm/s. The drag force value calculated in this literature is much smaller compared to the previous literature due to the lower magnetic force experienced by the MNPs.

### 2.3 Velocity Prediction in Confined Space

There are two mechanisms to describe the transportation of nanoparticles inside the narrow channel. Firstly, the particle does not experience a uniform velocity field on its surface, due to this behaviour, the velocity does not correlate to the fluid velocity in its centre (Liot et al., 2018). Then, the magnetophoretic of the particle in the steady-state can be calculated by using a simple force balance  $F_m = -F_D$ :

$$v = \frac{2\mu_0\rho_p M_p(H_a)r^2}{9\eta} \nabla H_a \quad (8)$$

Because of some restrictions we need to consider a laminar flow inside a rectangular pipe. (Liot et al., 2018) recently observed that there are two main regimes inside the confined channel from the transportation of the nanoparticles which are homogenous and inhomogeneous. The first regime, which is homogenous happens due to the ability of Brownian diffusion to homogenize the particle at pore entrance because of the factors small of the particle or high confinement. While for the inhomogeneous regime, it occurs at low Brownian diffusion and low confinement. To know the regime is homogenous or not, we need to find the  $\beta$ , which refers to the ratio of  $v_{exp} / v_{predicted}$ , in which  $v_{exp}$  refers to the experimented velocity while  $v_{predicted}$  is the predicted velocity. Theoretically, the homogenous regime belongs to the high confinement while the non-homogenous regime belongs to the high velocity of the fluid inside the microchannel.

Thus, it is believed that the regime inside the cellulose matrix is homogenous due to the high confinement (L.O. Mair, 2015) and the low velocity of the fluid (Call et al., 2020).

Based on (Jordi S. Andreu et al., 2012), we need to know the profile of the applied magnetic field and full characterization of the magnetic response,  $M_p(H_a)$  of the nanoparticles to use equation (8). It is assumed that  $M_p(H_a)$  of a single MNP under an external field,  $H$  is expressed within a good approximation by a Langevin function. Hence the  $M_p(H_a)$  can be expressed as

$$M_p H_a = M_s \mathcal{L}[b \mu_o H_a] \quad (9)$$

$M_s$  is the saturation magnetic moment per unit and  $\mathcal{L}$  is the Langevin function

$$\mathcal{L}[x] = \coth x - \frac{1}{x} \quad (10)$$

and  $b$  is related to  $M_s$  and  $r$  in which it can be written as

$$b = \frac{m_s}{K_B T} = \frac{4\pi r^3 M_s \rho_p}{3k_b T} \quad (11)$$

thus,  $x$  in equation (10) can be defined as

$$x = \frac{4\pi r^3 M_s \rho_p \mu_o H_a}{3k_b T} \quad (12)$$

Zachary D. and co in their recent study on isolating and detecting magnetic particles inside complex matrices (Call et al., 2020) have found that the minimum velocity of the fluids inside the microchannel with the maximum Reynolds number of 2 is at 67  $\mu\text{m/s}$ . The studies have been conducted with the three types of diameters of fluorescent carboxyl magnetic particles which are 2  $\mu\text{m}$ , 8  $\mu\text{m}$ , and 44.1  $\mu\text{m}$ .

## 2.4 Colloidal Stability

NP aggregation is a common phenomenon that can be observed in a complex environment (Moore et al., 2015). Aggregation is defined as the formation of large, irregularly shaped clusters of NPs because of usually irreversible inter-particle adherence. Aggregation of colloidal particles happens when physical processes bring particle surfaces into contact with one another and short-range thermodynamic interactions allow for particle-particle attachment (Zhang, 2014). Because of long-range Van Der Waals, VDWs and magnetic attraction among the particles, as well as the tendency of nanoscaled materials to aggregate into bulk to lower their surface energy, naked MNPs are likely to agglomerate quickly (Yeap et al., 2012). Few studies have found that smaller particles are more prone to aggregation at the same conditions due to interaction energy barrier decrease as particle decreases which means that as the energy barrier becomes smaller, the attachment efficiency of small NPs will increase (Zhang, 2014). (Call et al., 2020) in their study found that the lowest capture of MNPs was reported for the highest concentration due to NPs will aggregate at higher concentration. A similar phenomenon was observed in (Yeap et al., 2012) study in which even at a low concentration (6 mg/L), naked MNPs were extremely unstable. Within a few minutes of the ultrasonication process, the particles begin to flocculate into large clusters. The formation of aggregates can occur when stabilized NPs become unstable due to molecule/protein adsorption or loss of surface functionality (Moore et al., 2015).

Steric stabilizing agents are important to protect nanoparticles due to their sensitivity to the change of solution chemistry and may aggregate in certain aqueous environments (Lin & Wiesner, 2012). To avoid aggregation or to provide other related surface functionality, NPs are commonly stabilized with surface coatings to reinforce

the electrostatic, steric, or electrosteric repulsive force between NPs (Zhang, 2014). Surfactants, polymers, and polyelectrolytes are the three most common classes of surface coatings. The inter-particle behaviour caused by intermolecular and surface forces determines colloidal stability in which the colloidal stability of NPs in an aqueous suspension is determined by the balance of these two main forces (Moore et al., 2015). Poly(sodium 4-styrene sulfonate) coated MNPs of different molecular weights had studied by (Yeap et al., 2012). The magnetophoretic collection of MNPs was studied using a lab-scale high gradient magnetic separation (HGMS) device. It was found that PSS 70 kDa is a better stabilizer as compared to PSS 1000 kDa for the same concentration of NPs. This is due to the longer polymer chains in PSS 1000 kDa, which cause a less dense and extended PSS layer to form. Bridging flocculation was favoured by the extended polymeric chains, causing the coated particles to become less stable. Finally, the surface of MNPs is important in determining a particle's ability to avoid motion-inhibiting interactions with the matrix and move through the complex structure.

## **2.5 Capillary and Steric Force**

At the microscale, capillary forces can have a significant impact. At fluid-air-solid interfaces, capillary forces act to reduce the surface energy of the interface. The perimeter of the wetted area scales with surface tension or capillary forces (Lamkin-Kennard & Popovic, 2019). The capillary force is formed when ambient humidity condenses and forms a meniscus or liquid capillary neck between a particle and a surface. The capillary force also has a direct surface tension component, as surface tension pulls the contact line of the meniscus and the particle closer to the contact line of the meniscus and the surface. This force is defined as the surface tension force (Pakarinen et al., 2005). Several aspects influenced the capillary forces on the

nanoparticles such as the hydrophilic nature of adhering surfaces, ionic diffusion, the roughness of nanoparticles and substrate surface, the shape and size of the particle, kinetics of meniscus formation and deformation of the system (Harrison et al., 2015a).

The capillary pressure force and surface tension are the two components of the capillary force. The product of the pressure difference across the liquid-vapor interface and the wetter area of the particle is the capillary pressure force. The wetted perimeter of the particle is multiplied by the component of the surface tension normal to the two interacting surfaces to determine the surface tension force (Harrison et al., 2015b). Except for the highest humidities, the surface tension force is negligible. When spherical particles have a radius of 1  $\mu\text{m}$ , the surface tension force is negligible, but when the radius is 15 nm, it can be a larger component of the total capillary force than the capillary force pressure (Pakarinen et al., 2005).

Matrix fibres impose an additional steric force on particles in a gel network composed of connected fibrous proteins (L.O. Mair, 2015). The validation through direct observation of MNPs experiencing large inhibitory steric forces has been done in the experiment in which steric force imposed by the matrix plays a major role in inhibiting particle motion where steric force is one of the forces that influence the apparent viscosity other than drag force.

## **CHAPTER 3**

### **METHODOLOGY**

This chapter discloses the overall experimental aspects of the final year project. It includes the general research flow diagram, dynamical behavior calculations (drag force, drag force coefficient, Reynold numbers, and velocity), data of magnetophoretic dragging phenomenon of MNPs through cellulose matrix by using an optical microscope, and the data to identify the best working conditions for the magnetophoretic motion of MNPs along with cellulose matrix.

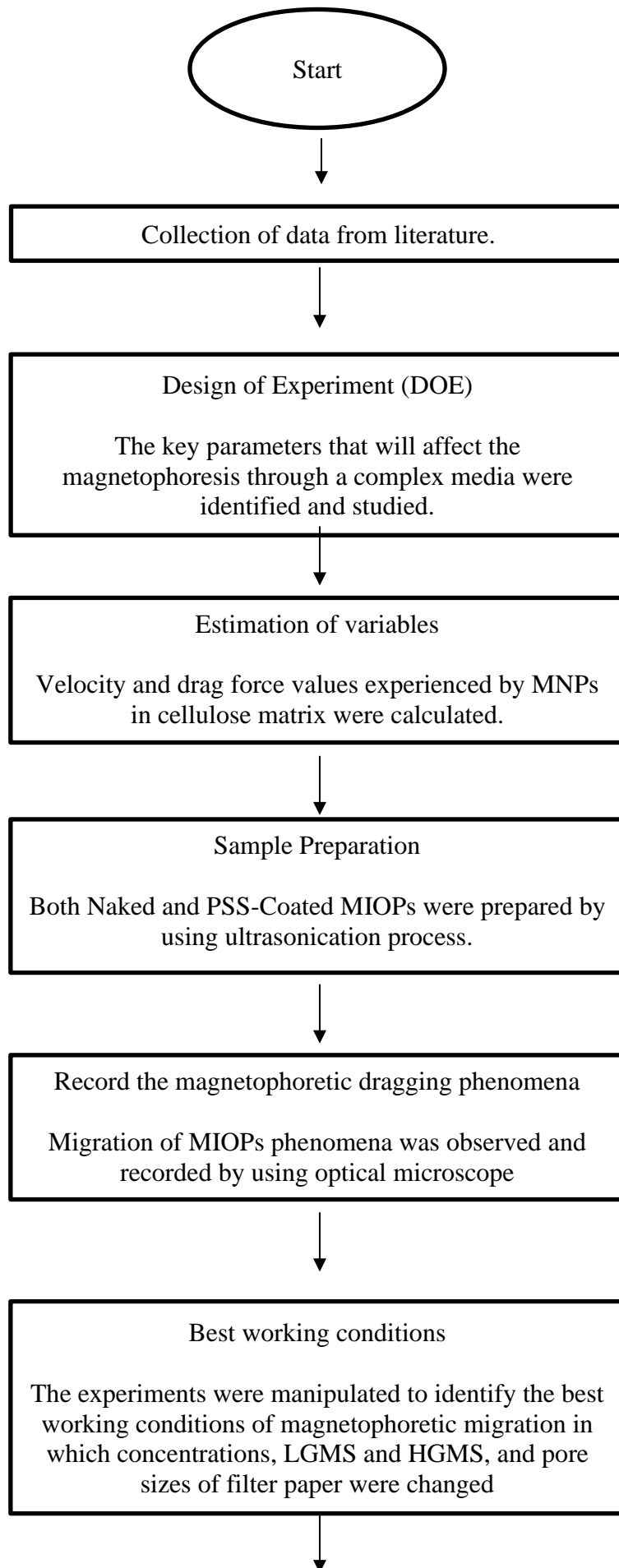
#### **3.1 Materials**

Whatman grade 4 and 5 chromatography paper were purchased from Sigma-Aldrich. A benchtop digital microscope was used to analyze the image. Water-soluble poly (sodium (4) styrene sulfonate) polyelectrolyte with ~70 000 Da (subsequently denoted as PSS 70k) was supplied by Sigma-Aldrich. Hydrochloric acid, HCl (Analytical reagent) obtained from Fischer Scientific. Cylindrical shaped N50-graded neodymium boron ferrite (NdBFe) permanent magnet with the surface magnetic field of ~6000 G was purchased from Ningbo YuXiang E&M Int'l Co., Ltd. A permanent bar magnet and stopwatch.

#### **3.2 Overview of Research Methodology**

Overall, this final year project focused on identifying the best working conditions of magnetophoresis through cellulose matrix.





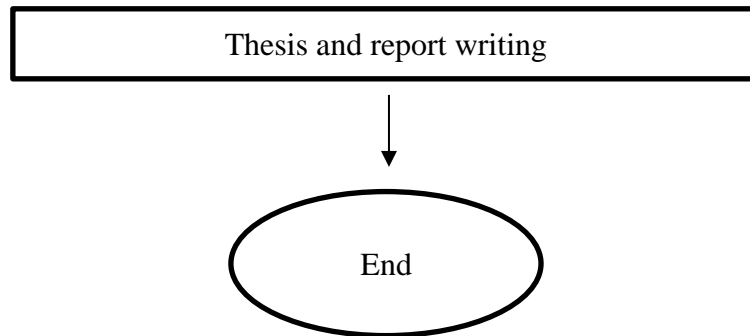


**Figure 3.1** Flow diagram of research project on magnetophoresis of MNPs through cellulose matrix

Drag force experienced by the MNPs whilst they move through cellulose matrix will be calculated using a modified form of Stoke's approximation for the case of drag on a spherical particle in which equation (4) will be used to calculate the value of the drag force. Due to the limitations of the experiment, all the parameters of the MNPs and the fluid inside the cellulose matrix will be extracted from the published literature. The parameters are the diameter of the MNPs, the viscosity of the fluid inside the cellulose matrix, density of MNPs, density of the fluid, and magnetic field. The magnetophoretic velocity also will be calculated by applying equation (8) in which will be the first step before proceeding with the drag force calculation.

To record the magnetophoretic dragging phenomena of MNPs, an optical microscope and with aid of software, Olympus cellSens will be used to analyze and record the magnetophoretic dragging phenomena of MNPs. The software can record the mobility of the magnetophoretic mobility since it can produce an analysis of the image based on its size, different dimensions of particles, and many more. All of the experiments were observed under the 10x view of an optical microscope and were analyzed by using ImageJ software.

### 3.3 Design of Experiment

In this thesis, Whatman grade 1 and grade 5 chromatography paper were cut into 8 pieces and then placed on top of a glass slide. Next, the whole piece of a cut chromatography paper was wetted with deionized water by using 10 mL of Transferpette. Introducing fluids onto the fiber is one of the ways to improve particle transport efficiency that largely influences an additional force provided by the fiber which is called the fiber drag force (Z. Xu et al., 2017). The grade N50 cylindrical permanent magnet was placed on top of the chromatography paper 2 cm away from the edge of the chromatography paper. A 1000 mg/L of  $\text{Fe}_3\text{O}_4$  nanoparticles were purchased from Sigma-Aldrich was diluted from 100 mg/L to 500 mg/L for the naked MNPs then ultrasonicated for 1 hour prior to use. 100 mg/L MNPs was diluted in Water-soluble poly (sodium (4) styrene sulfonate) polyelectrolyte for the coated MNPs. All of the MNPs solutions were labeled based on their concentration and type. After the ultrasonication process, 30  $\mu\text{L}$  of Transferpette was used to inject the MNPs onto the Whatman chromatography paper. A stopwatch was used to set the timer at 15,30 and 60 s after MNPs solution was injected. The permanent magnet was placed on top of the device 2 cm away and was optimized for consistent and ideal separation results based on magnetic field lines. Images of the MNPs on cellulose matrix were taken using cellSens software through the digital microscope. The images were taken for 0, 0.5, 1.0, 1.5, and 2.0 cm and were analyzed by using ImageJ. It has been reported from (Call et al., 2020) the analysis of particles captured was done after 30 s due to the fast-flow process has stopped after that time. The figure below shows the setup of the experiment followed by the information of Whatman chromatography paper used in the experiment.



**Figure 3.2:** Top view of the experiment setup

**Table 3.1** Properties of Whatman grade paper

	Grade 4	Grade 5
Particle's retention	25 $\mu\text{m}$	2.5 $\mu\text{m}$
Circles	27 mm – 400 mm	25 mm – 320 mm
Sheets	38 $\times$ 114 mm – 580 $\times$ 580 mm	
Nominal thickness	210 $\mu\text{m}$	200 $\mu\text{m}$

### 3.4 Velocity calculation

The parameters data of MNPs are tabulated in Table 3.2 in which all the data are extracted from the published literature

**Table 3.2:** Parameters of MNPs from published literature

Magnetic nanoparticles used	Diameter of a particle, 2r (nm)	Density particle, ( $\text{kg}/\text{m}^3$ )	Magnetic saturation	Reference
$\gamma$ - $\text{Fe}_2\text{O}_3$	12	4860	68 $\text{Am}^2/\text{kg}$	(Leong et al., 2020)
Beads	5000	2000	10 <sup>5</sup> A/m	(Gómez-Pastora et al., 2019)
$\gamma$ - $\text{Fe}_2\text{O}_3$	12	4860	68 $\text{Am}^2/\text{kg}$	(J S Andreu et al., 2011)
Core ( $\gamma$ - $\text{Fe}_2\text{O}_3$ ) / Shell ( $\text{SiO}_2$ )	82	2400	3. $\times$ 10 <sup>-18</sup> $\frac{\text{J}}{\text{T}}$	(J S Andreu et al., 2011)

Estapor M1-030/40	410	4860	45 kA/m	(Leong et al., 2020)
Fe <sub>3</sub> O <sub>4</sub>	65	5200	3.7 × 10 <sup>3</sup> A/m	(Lim et al., 2012)

To calculate the velocity of MNPs inside the cellulose matrix by using equation (8), we need to know the magnetic properties of the magnet used in our experiment. The magnetic properties such as magnetic field and gradient of the magnetic field are also extracted from the published literature. For the preliminary calculation, the gradient of the magnetic field will be less than 100 T/m (Leong et al., 2020; Schaller et al., 2008) in which the specific value is 30 T/m (LGMS) while the magnetic field will be 0.4-0.45 T.

Firstly, the value of  $x$  from equation 12 by using the data of Fe<sub>3</sub>O<sub>4</sub> from Table 3.2 is calculated

$$x = \frac{4\pi r^3 M_s \rho_p \mu_o H_a}{3k_b T}$$

Where

$$r = 32.5 \text{ nm} \quad \mu_o = 4\pi \times 10^{-7} \text{ H/m} \quad H_a = 0.4 \text{ T}$$

$$M_s = 3700 \text{ A/m} \quad k_b = 1.38 \times 10^{-23} \text{ J/K}$$

$$\rho_p = 5200 \text{ kg/m}^3 \quad T = 298 \text{ K}$$

$$x = \frac{4\pi(32.5 \times 10^{-9})^3 (3700)(5200)(4\pi \times 10^{-7})(0.4)}{3(1.38 \times 10^{-23})(298)}$$

$$x = 0.338 \frac{\text{kg}}{\text{m}^3}$$

then the calculated value of  $x$  is applied in the Langevin function, equation (10)

$$\mathcal{L}[x] = \coth x - \frac{1}{x}$$

$$\mathcal{L}[x] = \coth(0.338) - \frac{1}{(0.338)}$$